Edge effects on quantum thermal transport in graphene nanoribbons: Tight-binding calculations

Jinghua Lan,[1,*] Jian-Sheng Wang,[1,2] Chee Kwan Gan,[1] and Sai Kong Chin[1]
[1]*Institute of High Performance Computing, 1 Fusionopolis Way, #16-16 Connexis, Singapore 138632, Republic of Singapore*
[2]*Department of Physics and Center for Computational Science and Engineering, National University of Singapore, Singapore 117542, Republic of Singapore*
(Received 31 October 2008; published 3 March 2009)

We investigate the quantum thermal transport properties of graphene nanoribbons (GNRs) with natural edges by combining the Naval Research Laboratory tight-binding approach and the phonon nonequilibrium Green's function method. Thermal transport of GNRs shows substantial dependence on the width due to edge reconstructions. For GNRs with $n \geq 12$, where n is the number of atoms along the direction perpendicular to the ribbon axis, the effect of natural edges is negligible and quantized thermal transport is observed. For GNRs with $2 < n < 12$, natural edges destroy quantized thermal transport and reduce thermal conductance significantly. For the narrowest GNR with $n=2$, perfect quantized thermal transport is restored and a zero-transmission phonon band gap appears at $\omega = 785 \sim 808$ cm^{-1}. By sandwiching the narrowest GNR between two wide GNRs, the band gap is broadened by about ten times. The thermal conductivity of graphene evaluated from our results agrees very well with the recent experimental measurements.

DOI: 10.1103/PhysRevB.79.115401 PACS number(s): 68.65.−k, 44.10.+i, 63.20.kp

I. INTRODUCTION

Graphene has attracted considerable attention in recent years due to its versatile electronic properties[1–5] that are expected to be important for future nanoelectronics.[6] Interestingly, the electronic properties of graphene change in a nontrivial manner when going from bulk to nanometer size due to edge effects.[1,3,5] As the size of electronic devices decreases, the understanding of nanoscale thermal transport[7,8] becomes desirable for the miniaturization in the electronic devices. At nanoscale, the systems are of finite sizes and discrete, therefore continuum theories such as the Boltzmann equation will definitely not be suitable to describe such systems. One of the alternatives to the Boltzmann equation, the molecular-dynamics (MD) simulation based on atomic models, has been widely used to study a variety of carbon-based nanostructures.[7,8] However, since MD is a purely classical method, quantum effect cannot be taken into account.

Since geometric effects are important at nanoscale[9] and graphene nanoribbons (GNRs) have open structure at the edges, we expect to unveil thermal properties related to atomic details in GNRs explicitly by combining two approaches: the Naval Research Laboratory tight-binding (TB) (Ref. 10) method and the phonon nonequilibrium Green's function (NEGF) (Refs. 8 and 11) method. The nonorthogonal TB model has been shown to describe accurately the elastic constants and phonon dispersion of carbon systems.[12,13] We do not consider hydrogen passivation at the edges of GNRs or edge atoms at their perfect positions. However, we consider natural edges by performing atomic relaxation with the TB approach. Our consideration is realistic and reasonable since hydrogen atoms do not contribute much to thermal transport in carbon systems and natural reconstructions at edges always happen in real systems. Force constants are obtained with numerical finite differences by systematic displacement of each atom. Subsequently we use NEGF (Refs. 8, 14, and 15) method to calculate the thermal transport properties of different GNR-n, where n is the number of atoms along the direction perpendicular to the ribbon axis.

Due to natural edges, thermal transport properties of GNRs show significant dependence on their widths that can be described by n. We find that $n=12$ is the threshold width above which the effect of natural edges is negligible and quantized thermal transport is observed. Below the threshold width, natural edges destroy quantization of the transmission coefficient and reduce thermal conductance of GNRs. The thermal conductivity of a single-layered graphene evaluated from our conductance values and experimental mean-free-path value has a good agreement with the experimental measurements at room temperature. We find a zero-transmission band gap located at $\omega = 785 \sim 808$ cm^{-1} in the narrowest GNR with $n=2$ and the band gap is enlarged by a large factor of 10 when the GNR-2 is sandwiched between two wide GNRs leads.

The paper is organized as follows. In Sec. II we describe our model and numerical methods used for this study. In Sec. III we demonstrate and discuss the effect of edges on the thermal conductance of GNRs and the resulting width dependence. Comparison of calculated thermal conductivity for graphene with experimental measurements is provided in this section. Section IV is devoted to a sandwiched configuration of GNRs which exhibits unusual thermal transport properties. Conclusions are found in Sec. V.

II. MODEL AND METHODOLOGY

We consider a junction connected to two semi-infinite long leads. The junction is the central part (labeled as C) and the two leads are the left (L) and right regions (R). The Hamiltonian[8,15] is given by

$$H = \sum_{\alpha=L,C,R} H_\alpha + (u^L)^T V^{LC} u^C + (u^C)^T V^{CR} u^R, \qquad (1)$$

where $H_\alpha = \frac{1}{2}(\dot{u}^\alpha)^T \dot{u}^\alpha + \frac{1}{2}(u^\alpha)^T K^\alpha u^\alpha$ represents coupled harmonic oscillators, u^α is the mass-normalized displacement in

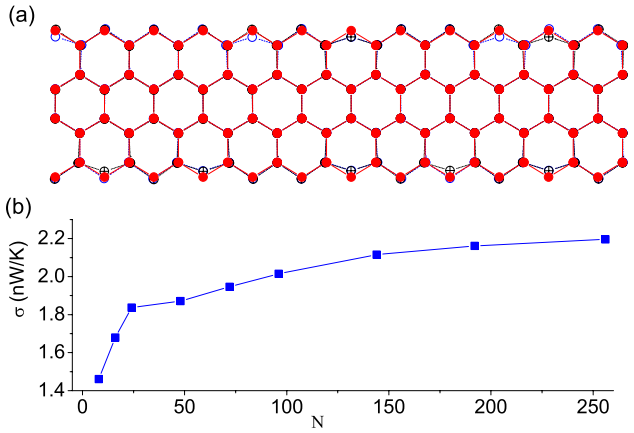

FIG. 1. (Color online) (a) Configuration of different GNR-4. Full circles represent the configuration of the perfect GNR-4. Circles with and without "+" represent two configurations after relaxation. (b) Thermal conductance σ of perfect GNR-4 at 300 K versus the number of atoms N in the center region. N takes $2n$, $4n$, $6n$, $12n$, $18n$, $24n$, $36n$, $48n$, and $64n$.

region α, and $\dot{u}^{\alpha}$ is the corresponding conjugate momentum. K^{α} is the spring constant matrix and $V^{LC}=(V^{CL})^{T}$ is the coupling matrix between L and C regions; similarly for V^{CR}. The semi-infinite left and right regions have perfect periodicity along the ribbon axis and are assumed to be at different equilibrium heat-bath temperatures. We should point out that Eq. (1) takes into account three-dimensional vibrational modes. This differs from a recent work[16] in which out-of-plane modes are considered

We cut a GNR with zigzag edges from an infinite graphene sheet at its lowest-energy state and relax the system to its minimum-energy configuration using the TB method.[10] Here we only consider GNRs with zigzag edges because they have stable energy states after relaxation. GNRs with armchair edges are very unstable during structural minimization and only metastable states can be found when hydrogen atoms are not passivated at armchair edges.[17] We find that the narrowest ribbon, GNR-2, is quite stable as its configuration remains unchanged after relaxation. However, GNRs-n configurations with $n>2$ experience significant changes near the edges after relaxation. These observations are demonstrated in Fig. 1(a) where three configurations of GNR-4 are included. One corresponds to the perfect GNR-4 and two are obtained after relaxations from different initial configurations. The two final states have different configurations as shown in Fig. 1(a), but they have almost the same energy with an energy difference $|E_1^f-E_2^f|=0.07$ eV/(96-atom).

We perform first-principles calculations with Vienna *ab initio* simulation package (VASP) (Ref. 18) to confirm our TB observations in GNR-4. Comparison of results obtained with these two methods are presented in Table I. The difference in C-C bond length is about 1.2%. As shown in Table I, the final energy difference for two perturbed GNR-4 with VASP calculations is also small, $|E_1^f-E_2^f|=0.14$ eV/(96-atom). Reconstruction at the edges is also observed using VASP, which is consistent with the results from TB method.

After performing the relaxation, we subject the GNR system to individual atomic displacement and evaluate the resulting forces on all atoms. Repeating the process for each atom, the force constants are then evaluated using a central-difference scheme. We use a reasonably small maximum displacement of 3×10^{-4} Å which is 2 orders of magnitude smaller than that commonly used in a supercell force-constant method.[19]

The ballistic thermal conductance of a junction connected to two leads at different equilibrium heat-bath temperatures is given by the Landauer formula,

$$\sigma(T)=\int_0^{\infty}\frac{d\omega}{2\pi}\hbar\omega T[\omega]\frac{\partial f}{\partial T}, \tag{2}$$

where $f=\{\exp[\hbar\omega/(k_BT)]-1\}^{-1}$ is the occupation distribution function for heat carriers at the reservoirs, and $T[\omega]$ is the transmission coefficient (or transmittance). For ideal quasi-one-dimensional periodic systems, $T[\omega]$ is just the number of phonon branches at frequency ω at low temperatures, i.e., the thermal transport is quantized at the universal value, $\sigma_0=\pi^2k_B^2T/3h$, for periodic systems.[11,20] When the system is not perfectly periodic, several other approaches can be used to calculate the transmission (see Ref. 8). In this paper, we use phonon NEGF method through the Caroli formula to compute the transmission coefficient,

$$T[\omega]=\mathrm{Tr}(G^r\Gamma_L G^a\Gamma_R), \tag{3}$$

where $G^r=(G^a)^{\dagger}=[(\omega+i\eta)^2-K^C-\Sigma_L^r-\Sigma_R^r]^{-1}$ is the retarded Green's function for the center region, while $\Gamma_{\alpha}=i(\Sigma_{\alpha}^r-\Sigma_{\alpha}^a)$ describes the interaction between the leads and the central region. The retarded self-energy of the leads is given by $\Sigma_{\alpha}^r=V^{C\alpha}g_{\alpha}^rV^{\alpha C}$, where

$$g_{\alpha}^r=[(\omega+i\eta)^2I-K^{\alpha}]^{-1} \tag{4}$$

is the retarded surface Green's function for the leads. As we can see, the transmission coefficient can be obtained if we know the surface Green's function g_{α}^r which can be obtained from Eq. (4). The thermal conductivity of a finite sample is

TABLE I. Comparison of C-C bond length and reconstruction energy by VASP calculations and TB method. We consider two slightly randomly perturbed GNR-4 with 96 atoms per supercell. E_1^i and E_2^i (with unit eV) are the total energies of the initial states. E_1^f and E_2^f (with unit eV) are the total energies of the final states. ΔE_1 and ΔE_2 are the energy difference between the final states and the initial states. For easy comparisons, the total energies have been shifted in such a way that E_1^i are zero for VASP and TB calculations.

Methods	a_0(Å)	E_1^i	E_1^f	ΔE_1	E_2^i	E_2^f	ΔE_2
DFT	1.412	0	−3.636	−3.636	1.986	−3.775	−5.761
TB	1.425	0	−4.275	−4.275	2.510	−4.350	−6.860

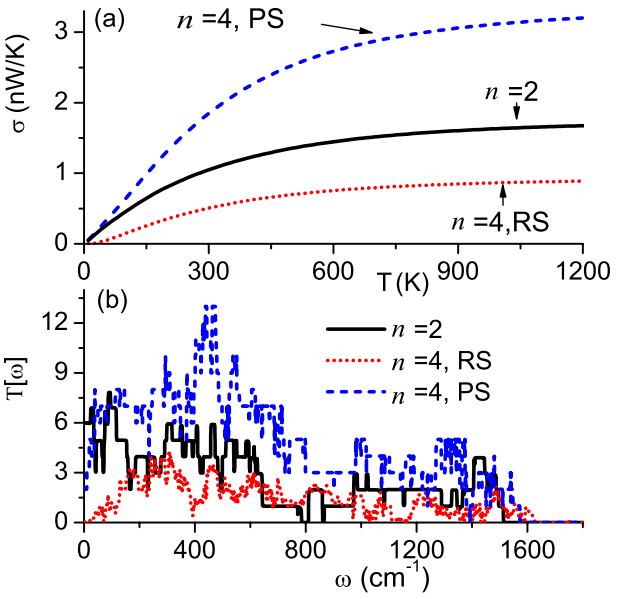

FIG. 2. (Color online) Transport properties of GNRs with width $n=2$ and $n=4$. Dotted curve corresponds to the case for the relaxed structure (RS) of GNR-4 and dashed curve corresponds to the case for the perfect structure (PS) of GNR-4. (a) Thermal conductance of GNR-2 and GNR-4. (b) Transmission of GNR-2 and GNR-4.

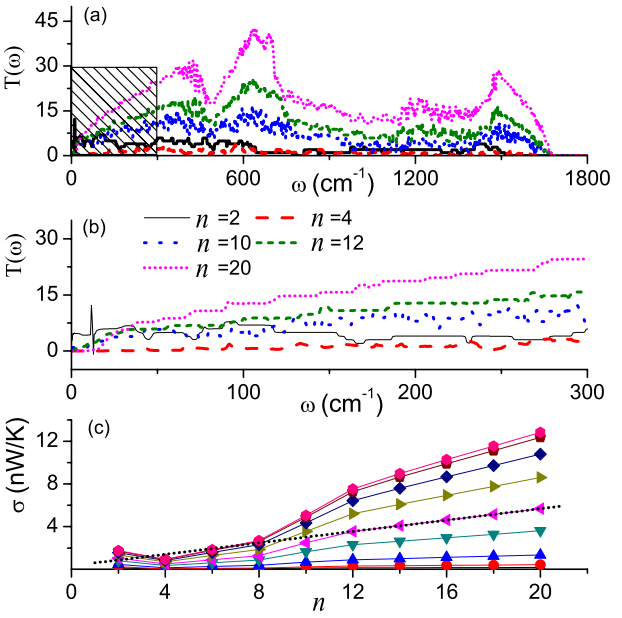

FIG. 3. (Color online) (a) Transmission of GNR-n with $n=2$, 4, 10, 12, and 20. (b) Enlarged from the shaded region in (a). (c) Thermal conductance versus GNRs' width n at temperatures 50, 100, 200, 300, 500, 800, 1500, and 2500 K from bottom to top. The dotted line is a fitting curve for $n \geq 12$ at 300 K.

related to its conductance by $\kappa=\sigma l/S$, where l is the length of the suspended segment of the graphene, and S is its cross section. Since the cross section is not well defined in GNRs, we will discuss the results in terms of conductance.

Our phonon NEGF approach is essentially a generalization of the fermionic NEGF method[21] to the case of bosons. The generalization is discussed in details in Refs. 8 and 15. The NEGF formalism provides powerful means to handle open quantum systems that are not confined but connected to reservoirs. This technique is promising for a truly first-principles approach and it appears to give excellent results up to room temperatures.[15]

In our investigation, the default length of the central part is 7.4 Å ($3\sqrt{3}a_0$, where a_0 is the C-C bond length). The number of atoms in this default length is $6n$. Since the relevant interaction in our system is long ranged, thermal conductance is expected to increase with system size and converge to a constant in the bulk limit. This expectation is confirmed in Fig. 1(b). Thermal conductance σ increases with the system size N monotonously. However, the increment becomes gradual after $N>6n$. Hereafter, we employ $6n$ as a suitable size to predict thermal conductance in GNRs. Note that if we set a cut-off distance L_c for interaction, σ will remain the same when the system size is larger than L_c.

III. EDGES EFFECT ON THERMAL TRANSPORT OF GNRS

Figure 2 compares the transmission $T[\omega]$ and thermal conductance σ for GNR-2 and GNR-4. The full curve in Fig. 2 shows the transport properties of the GNR-2, which is the most stable, without distortion at the edges. Its transmission exhibits a stepwise structure that reflects the number of phonon modes in the corresponding frequency regions. In this case, the propagating phonons in each mode are not scattered and they are transmitted perfectly through the GNR-2. Thus, the thermal conductance is quantized as the universal value at low temperatures from Eq. (2). In particular, we observe a narrow zero-transmission band located at $\omega=785\sim808$ cm^{-1} in which no phonon contributes to the thermal current. This zero-transmission band only exists in GNR-2 which is the narrowest GNR with zigzag edges. However quantized thermal transport is destroyed in a relaxed GNR-4 which has random edges [see the dotted curve in Fig. 2]. The corresponding σ is very small. In contrast, the thermal transport properties of a perfect GNR-4 are plotted [see the dashed curve in Fig. 2]. Steplike $T[\omega]$ of the perfect GNR-4 is distinct in Fig. 2(b) and the corresponding σ is much higher than that of the relaxed GNR-4 as shown in Fig. 2(a).

As the GNR width increases from $n=4$, the transmission $T[\omega]$ and σ increase monotonously as shown in Fig. 3. An interesting phenomenon is that for $n \geq 12$, quantized thermal transport is restored. The reemergence of steplike features of $T[\omega]$ can be seen clearly in Figs. 3(a) and 3(b). Therefore, $n=12$ can be identified as the threshold width above which the effect of natural edges is negligible and quantized thermal transport is expected. This expectation is confirmed in Fig. 3(c) in which σ depends linearly on the width of GNRs for $n \geq 12$. This is physically consistent with the fact that within quantized thermal transport regime, the number of phonon modes (and hence σ) depends linearly on the number of atoms in the GNR, and hence n. The width threshold $n=12$ suggests a suitable width of GNR in order to explore thermal properties of graphene. Using our σ value with $n \geq 12$ and the experimental mean-free-path

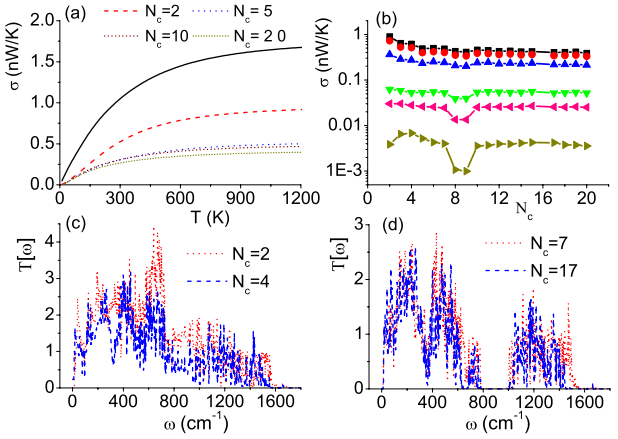

FIG. 4. (Color online) (a) Thermal conductance of the sandwiched device versus temperature for different numbers of cells N_c in the central region. For comparison, the full line corresponds to the conductance of an infinite GNR-2. (b) Thermal conductance versus the number of cells N_c at temperatures 10, 30, 50, 200, 500, and 1000 K from bottom to top. (c) Transmission of the sandwiched device with N_c equal to 2 and 4. (d) Transmission of the sandwiched device with N_c equal to 7 and 17.

value $\bar{L}=775$ nm,[22] we can evaluate the thermal conductivity of graphene with the relation $\kappa=\sigma\bar{L}/S$. We find that at room temperature $\kappa=3410$ W/mK, which agrees well with the recent experimental measurements of $\kappa=3080 \sim 5150$ W/mK in graphene.[22]

IV. THERMAL PROPERTIES OF SANDWICHED GNRS

In this section, we consider a nanostructure in which a GNR-2 with finite length is sandwiched between two wide semi-infinite GNRs ($n \geq 12$). This structure is similar to a one-dimensional chain connected with two bulk leads. The length of the center GNR-2 is characterized by N_c: the number of basis unit cells. This simple structure exhibits unusual thermal transport properties and it may be used as a device as shown below.

First, the device generally has a small thermal conductance compared to an infinite GNR-2 as shown in Fig. 4(a) and σ has a dependence on the length N_c of the central region as shown in Fig. 4(b). The conductance σ has a valley around $N_c=8 \sim 9$ and σ depends sensitively on N_c at low temperatures. When the temperature increases to over 50 K, the valley disappears and σ decreases slowly as N_c increases. The conductance σ is expected to converge to a constant at a certain temperature as N_c increases continuously. The length dependence of σ in this sandwiched device is opposite to the observation in Fig. 1(b). But they are not incompatible. For an infinite perfect structure which is produced by aligning the central part periodically in general NEGF models, phonons transfer without scattering. As N_c increases, additional phonons with long wavelengths contribute to thermal conductance. However for the sandwiched device, there are two interfaces that scatter phonons from the central part and significantly suppress thermal conductance. As the junction size increases, more phonons are scattered by the interfaces and the corresponding thermal conductance decreases. Other groups also found similar length dependence of thermal transport through one-dimensional alkane chains connected with bulk materials.[23]

Second, $T[\omega]$ changes from a continuous band to a split band with a wide gap at 780 $\text{cm}^{-1} < \omega < 1000$ cm^{-1} for $N_c > 5$ as shown in Figs. 4(c) and 4(d) with selected N_c. Within the band gap, no phonon of that frequency can be transmitted through the device. This wide band gap is quite robust as it remains at the same width and at the same location for $N_c = 5 \sim 20$. But the band gap will immediately disappear if we replace the GNR-2 with other GNRs. We suggest that the wide band gap extended from the intrinsic band gap in GNR-2 is due to the strong scattering from the interfaces. When $2 \leq N_c \leq 4$, all atoms at the central region have good coupling with the leads. In this case, overlaps of different phonon branches result in a continuous transmission in whole ω space. However, when $N_c \geq 5$ the strong scattering from the leads results in the disappearance of vibration modes in the range 780 $\text{cm}^{-1} < \omega < 1000$ cm^{-1}. This particular range is always found to have a relatively small transmission for any carbon-based systems. If we consider the nonlinear interactions in GNRs, the effective transmission should depend on temperature according to the vibrational band studies in Ref. 24. This opens the possibility of manipulating thermal transport[24] or phononic waves[25] through nanodevices based on GNRs.

V. CONCLUSIONS

In summary, the effect of natural edges plays a substantial role on thermal transport of GNRs. The natural edges result in strong width dependence of thermal transport for different GNRs. By sandwiching the narrowest GNR between two wide GNRs, we have shown the possibility of manipulating phonon band gap in such nanostructures.

ACKNOWLEDGMENT

J.-S.W. acknowledges support from the Academic Research Fund of NUS under Grant No. R-144-000-173-101/112.

*lanjh@ihpc.a-star.edu.sg

[1] K. Nakada, M. Fujita, G. Dresselhaus, and M. S. Dresselhaus, Phys. Rev. B **54**, 17954 (1996).

[2] D. A. Abanin, P. A. Lee, and L. S. Levitov, Phys. Rev. Lett. **96**, 176803 (2006).

[3] Y.-W. Son, M. L. Cohen, and S. G. Louie, Phys. Rev. Lett. **97**, 216803 (2006).

[4] A. K. Geim and K. S. Novoselov, Nature Mater. **6**, 183 (2007).

[5] J. H. Lee, J. Balasubramanian, R. T. Weitz, M. Burghard, and K. Kern, Nat. Nanotechnol. **3**, 486 (2008).
[6] L. Chico, V. H. Crespi, L. X. Benedict, S. G. Louie, and M. L. Cohen, Phys. Rev. Lett. **76**, 971 (1996).
[7] D. G. Cahill, W. K. Ford, K. E. Goodson, G. D. Mahan, A. Majumdar, H. J. Maris, R. Merlin, and S. R. Phillpot, J. Appl. Phys. **93**, 793 (2003); S. Lepri, R. Livi, and A. Politi, Phys. Rep. **377**, 1 (2003).
[8] J.-S. Wang, J. Wang, and J. T. Lü, Eur. Phys. J. B **62**, 381 (2008).
[9] P. Koskinen, H. Häkkinen, B. Huber, B. von Issendor, and M. Moseler, Phys. Rev. Lett. **98**, 015701 (2007).
[10] M. J. Mehl and D. A. Papaconstantopoulos, Phys. Rev. B **54**, 4519 (1996).
[11] T. Yamamoto, S. Watanabe, and K. Watanabe, Phys. Rev. Lett. **92**, 075502 (2004).
[12] D. A. Papaconstantopoulos, M. J. Mehl, S. C. Erwin, and M. R. Pederson, *Tight-binding approach to computational material science*, edited by P. E. A. Turchi, A. Gonis, and L. Colombo, MRS Symposia Proceedings No. 491 (Materials Research Society, Pittsburgh, 1998), p. 221.
[13] M. G. Fyta, I. N. Remediakis, P. C. Kelires, and D. A. Papaconstantopoulos, Phys. Rev. Lett. **96**, 185503 (2006).
[14] N. Mingo and L. Yang, Phys. Rev. B **68**, 245406 (2003).
[15] J.-S. Wang, J. Wang, and N. Zeng, Phys. Rev. B **74**, 033408 (2006); J.-S. Wang, N. Zeng, J. Wang, and C. K. Gan, Phys. Rev. E **75**, 061128 (2007).
[16] M. Morooka, T. Yamamoto, and K. Watanabe, Phys. Rev. B **77**, 033412 (2008).
[17] P. Koskinen, S. Malola, and H. Häkkinen, Phys. Rev. Lett. **101**, 115502 (2008).
[18] G. Kresse and J. Furthmüller, Phys. Rev. B **54**, 11169 (1996).
[19] C. K. Gan, Y. P. Feng, and D. J. Srolovitz, Phys. Rev. B **73**, 235214 (2006).
[20] L. G. C. Rego and G. Kirczenow, Phys. Rev. Lett. **81**, 232 (1998); K. Schwab, E. A. Henriksen, J. M. Worlock, and M. L. Roukes, Nature (London) **404**, 974 (2000).
[21] Y. Meir and N. S. Wingreen, Phys. Rev. Lett. **68**, 2512 (1992).
[22] S. Ghosh, I. Calizo, D. Teweldebrhan, E. P. Pokatilov, D. L. Nika, A. A. Balandin, W. Bao, F. Miao, and C. N. Lau, Appl. Phys. Lett. **92**, 151911 (2008); Nano Lett. **5**, 1842 (2006).
[23] D. Segal, A. Nizan, and P. Hänggi, J. Chem. Phys. **119**, 6840 (2003); Z. Wang, J. A. Carter, A. Lagutchew, Y. K. Koh, N.-H. Seong, D. G. Cahill, and D. D. Dlott, Science **317**, 10 (2007).
[24] J. Lan and B. Li, Phys. Rev. B **75**, 214302 (2007); B. Li, J. H. Lan, and L. Wang, Phys. Rev. Lett. **95**, 104302 (2005).
[25] T. Gorishnyy, C. K. Ullal, M. Maldovan, G. Fytas, and E. L. Thomas, Phys. Rev. Lett. **94**, 115501 (2005).